

# Relating Spatially Resolved Maps of the Schottky Barrier Height to Metal/Semiconductor Interface Composition

Robert Balsano, Chris Durcan, Akitomo Matsubayashi, and Vincent P. LaBella\*

*College of Nanoscale Science and Engineering,*

*University at Albany, SUNY, Albany, New York 12203, USA*

(Dated: August 28, 2021)

## Abstract

The Schottky barrier height (SBH) is mapped with nanoscale resolution at pure Au/Si(001) and mixed Au/Ag/Si(001) interfaces utilizing ballistic electron emission microscopy (BEEM) by acquiring and fitting spectra every 11.7 nm over a  $1 \mu\text{m} \times 1 \mu\text{m}$  area. The energetic distribution of the SBH for the mixed interfaces contain several local maximums indicative of a mixture of metal species at the interface. To estimate the composition at the interface, the distributions are fit to multiple Gaussians that account for the species, “pinch-off” effects, and defects. This electrostatic composition is compared to Rutherford backscattering spectrometry (RBS) and x-ray photo-emission spectroscopy (XPS) measurements to relate it to the physical composition at the interface.

---

\*Electronic address: vlabella@albany.edu; Present Address: SUNY Polytechnic Institute, Albany, New York 12203, USA

## I. INTRODUCTION

Metal/semiconductor interfaces form rectifying Schottky contacts, widely utilized in power applications due to their low turn on voltages and high switching speeds. Schottky diodes are also found in sensor applications as both gas and optical sensors due in part to their simplicity [1, 2]. In addition, Schottky source/drain contacts are being utilized in sub 20 nm node transistors to improve scalability [3–8]. This motivates the need to study and understand the nanoscale fluctuations in the Schottky barrier height at metal semiconductor interfaces [9–12].

The Schottky barrier height (SBH) is the energy offset of the conduction band minimum in the semiconductor with respect to the metal’s Fermi level resulting from the bare space charge that exists at the interface and within the semiconductor. The barrier height is dependent upon the type of metal and semiconductor as well as interface states and bonding, which can be altered by the fabrication process such as surface pre-treatments, or unintentional foreign species [13, 14]. These effects can vary locally and can cause inhomogeneities in the barrier height [15–21]. Electrostatic models that explain SBH inhomogeneity predict that a region of metal with a lower barrier height will have its barrier height increased when it is surrounded by a metal with a higher barrier height for a given semiconductor substrate [9–13]. This is dubbed *pinch-off* and is a function of the size of the surrounded region of metal in relation to the depletion width of the diode. This is in part a consequence of the continuity in the electrostatic potential at the interface as it will vary smoothly across regions with different metals that exhibit different barrier heights [9–12].

Fluctuations in the barrier height at the nanoscale can only be examined utilizing ballistic electron emission microscopy (BEEM), which is a powerful technique to measure local Schottky barrier heights with nanoscale resolution [22–24]. It is a three terminal scanning tunneling microscopy (STM) technique where the STM tip is used to locally inject tunneling electrons into a grounded metal film deposited onto the surface of a semiconductor as shown schematically inset in Fig. 2(a) [22–24]. Electrons with energy greater than the SBH are collected at the semiconductor and measured as BEEM current as depicted inset in Fig. 2(b). Mapping of the SBH is achieved by fitting the spatially resolved transmission as a function of tip bias to extract the local SBH at individual tip locations and can achieve nanoscale resolution [15–21].

Several studies have mapped the SBH using BEEM. Palm et al. took a series of 12 BEEM images of varying tip bias over a  $60 \text{ nm} \times 60 \text{ nm}$  area on the Au/Si(100) and Au/Si(111) interfaces and did a pixel by pixel fit to generate a SBH map [19, 21]. Olbrich et al. created SBH maps of a mixed Au/Co/GaAs interface consisting of small Co grains enveloped by Au on a  $114 \text{ nm} \times 114 \text{ nm}$  area sampling every  $0.89 \text{ nm}$  where pinch off effects were observed [15, 16]. Goh et al. mapped SBHs of an Au/pentacene/Si(111) interface using a  $30 \times 30$  point grid of spectra taken every  $17 \text{ nm}$  [17]. Durcan et al. mapped the W/Si(001) interface with *p*-type and *n*-type substrates over a  $1 \mu\text{m} \times 1 \mu\text{m}$  area sampling every  $11.7 \text{ nm}$  [20]. However, no studies have measured the Schottky interface of mixed Au and Ag on the Si(001) substrate, which would be insightful for *pinch-off* effects due to the large differences in their barrier height's ( $\sim 0.2 \text{ eV}$ ) and their miscibility [25].

In this article, the SBH for Ag and Au mixed films on Si(001) are mapped with nanoscale resolution by acquiring 7,225 spectra in a regularly spaced grid over a  $1 \mu\text{m} \times 1 \mu\text{m}$  area. False color spatial maps and energy histograms of the SBH are utilized to relate the electrostatic character of the interface to its material composition. The distributions are fit to a sum of Gaussian distributions arising from the presence of multiple species at the interface, “pinch-off” effects, and interface defects. The composition obtained from this fitting is corroborated with depth resolved chemically sensitive techniques.

## II. EXPERIMENTAL

The Schottky diodes were fabricated under ultra high vacuum (UHV) using *n*-type single crystal Si(001) wafers with a resistivity of  $100 \Omega\text{-cm}$  (phosphorus doped). The native oxide layer was removed utilizing a standard chemical hydrofluoric acid treatment immediately prior to loading into a UHV ( $10^{-10} \text{ mbar}$ ) chamber [26, 27]. The metal films were deposited onto the silicon surface using standard Knudsen cells through a  $2 \text{ mm} \times 1 \text{ mm}$  shadow mask. Three samples were fabricated with  $0 \text{ nm}$ ,  $1 \text{ nm}$ , and  $30 \text{ nm}$  thick silver layers while the gold capping layer was kept at  $7.5 \text{ nm}$  thick for all samples. Each diode was mounted onto a custom designed sample holder for BEEM measurements. The holder allowed for the metal film to be grounded using a BeCu wire and connection of the silicon substrate to the ex situ pico-ammeter to measure the BEEM current. Ohmic contacts were established by cold pressing indium into the backside of the silicon substrate.

A modified low temperature UHV STM (Omicron) was utilized for all BEEM measurements with a pressure in the  $10^{-11}$  mbar range [28]. The samples were inserted into the UHV chamber and loaded onto the STM stage that was cooled to 80 K for all measurements. Two-point current-voltage measurements were taken *in situ* with BEEM measurement for each sample at low temperatures without ambient light using a Keithley 2400 source measurement unit to verify rectifying behavior. Pt/Ir STM tips, mechanically cut at a steep angle, were utilized for all BEEM measurements. BEEM spectra were acquired using a constant tunneling current setpoint of 1 nA for the the sample with no silver and 30 nm of silver, while 30 nA was utilized for the sample with 1 nm of Ag. All BEEM spectra were acquired over a tip bias range of 0.20 eV to 2.00 eV at 80 K. A spectrum was taken every 11.7 nm over a  $1 \mu\text{m} \times 1 \mu\text{m}$  area of the metal surface, resulting in 7,225 spectra for each sample.

Each individual spectrum and the average of all spectrum for each sample were fit to the simplified Bell and Kaiser (BK) model,  $I_B \propto (\phi_b - V_t)^n$ , where  $I_B$  is the BEEM current,  $\phi_b$  is the SBH,  $V_t$  is the tip bias, and  $n = 2$  is the fitting exponent utilizing a linearization technique [25]. The fitting returned a SBH along with the  $R^2$  value as an indicator of the quality of the fit. SBH spatial maps and energetic histograms for the individual spectra were generated from these fits. Rutherford backscattering spectrometry (RBS) was performed to measure film thickness and composition analysis. An x-ray photo-emission spectroscopy (XPS) sputter depth profile was performed on the sample with the 1 nm Ag layer.

### III. RESULTS

XPS sputter depth profiles as a function of time for the 7.5 nm Au/30 nm Ag/Si and 7.5 nm Au/1 nm Ag/Si samples are displayed in Fig. 1 and show the presence of Ag, Au, and Si in the diode. The composition at the interface is taken to be the composition just before silicon is detected. In the 30 nm Ag sample, Ag is the dominant species with 95% at the interface and about 5% Au. In the 1 nm Ag sample, Au is the dominant species with 85% at the interface and about 15% Ag.

The averaged BEEM spectra for the three samples are displayed in Fig. 2. Each spectrum shows an onset threshold characteristic of a Schottky barrier at the interface. The averaged spectrum and its fit are shown in raw and linearized forms indicating the SBH and  $R^2$  value in Fig. 3. The data is indicated by a blue line, the region of fit is indicated by a solid red line,

and the extrapolation from the region of fit to the  $x$ -axis intercept or SBH is indicated by a dotted red line. Visible in the fits is the large difference in the region of extrapolation from sample to sample where the Au/Ag samples, Fig. 3 (e) and Fig. 3 (f) have extrapolation regions of about 0.14 eV which is larger than the pure Au sample seen in Fig. 3 (b).

The SBHs resulting from fitting each spectrum for all three samples are displayed as a false color spatial maps (left) and an energetic histogram (right) in Fig. 4 (a)-(c). A small square is shown in the bottom left corner to indicate the pixel size of each individual spectrum. The black pixels indicate a spectrum that could not be fit, while white pixels indicates a spectrum with a SBH above the upper limit of the scale. The histograms for all distributions are plotted from 0.40 eV to 1.80 eV, spanning the range of values obtained from fitting and display the average  $R^2$  values of the data sets. A scatter plot of the SBH as a function of  $R^2$  value is displayed in the inset of each histogram. The horizontal and vertical dotted lines mark the average barrier height and  $R^2$  value, respectively. The majority of points surround the intersect of the two averages and indicate that high barrier heights have high  $R^2$  values.

The spatial distribution of the fitted SBHs for the 7.5 nm Au/Si sample are displayed in Fig. 4 (a). The map displays a spatially homogeneous barrier height near 0.86 eV with a few regions where no fit was obtained and several high barrier regions outside of the color scale. The histogram indicates a very narrow distribution of barrier heights extracted from a total of 7,217 spectra. The mean barrier height is 0.87 eV with a standard deviation of 0.024 eV. The barrier height of the average spectrum, 0.86 eV is indicated with the vertical red dotted line.

The spatial distribution of SBHs from the 7.5 nm Au/30 nm Ag/Si diode are displayed in Fig. 4 (b). The map displays a spatially mixed distribution of barrier heights with a small number of locations where no fit was obtained and several high barrier regions outside of the color scale. A large portion of the image has a barrier height between 0.70 eV and 0.80 eV. There are also many regions that exhibit a barrier height near 0.86 eV. The histogram depicts a broad mixture of barrier heights from 7,224 spectra. The mean barrier height is 0.78 eV with a standard deviation of 0.103 eV. The barrier height from the fit to the average spectrum, 0.73 eV is lower than the mean and indicated with the vertical red dotted line.

The spatial distribution of SBHs for the 7.5 nm Au/1 nm Ag/Si sample are displayed in Fig. 4 (c). The map displays a spatially inhomogeneous distribution of SBHs with a few

regions where no fit was obtained and a number of high barrier regions outside of the color scale. There are small patches with SBHs below 0.80 eV, but the surrounding area is mostly between 0.80 eV and 0.90 eV. The histogram indicates 7,224 spectra were able to be fit with the distribution having multiple local maximums. The mean barrier height is 0.83 eV with a standard deviation of 0.109 eV. The barrier height from the fit to the average spectrum, 0.85 eV is higher than the mean and indicated with a vertical red dotted line.

Histograms depicting the BEEM data for the 7.5 nm Au/30 nm Ag/Si (a) and 7.5 nm Au/1 nm Ag/Si (b) samples are shown in Fig. 5. The histogram in (a) illustrates a multi-modal fit to the distribution in green with its constituent normal distributions drawn in black. The means of the five centroids are indicated by red dotted lines, are 0.62 eV, 0.73 eV, 0.76 eV, 0.86 eV, and 1.00 eV, and contribute 4.0%, 5.0%, 72.5%, 14.5%, and 4.0% to the multi-modal distribution with standard deviations 0.057 eV, 0.010 eV, 0.053 eV, 0.067 eV, and 0.067 eV, respectively. The histogram in (b) illustrates a multi-modal fit to the distribution in green with its constituent normal distributions drawn in black. Red dotted lines indicate the distribution means of 0.62 eV, 0.69 eV, 0.75 eV, 0.85 eV, and 0.94 eV, contribute 3.5%, 7.0%, 16.0%, 58.0%, and 15.5% to the multi-modal distribution and have standard deviations 0.041 eV, 0.031 eV, 0.041 eV, 0.036 eV, and 0.072 eV, respectively.

#### IV. DISCUSSION

The SBH obtained for the Au sample is in good agreement with the previously reported values, but the SBHs for the silver samples are not in agreement with the reported value of 0.66 eV [25]. The SBH of the average spectrum for the 30 nm Ag sample is over 50 meV higher and almost 200 meV higher for the 1 nm Ag sample. In addition, the 13 meV width of the extrapolation region for the linearized fits for both Ag samples and the underestimation of the fit line in the raw spectra indicate that single threshold fitting is not appropriate. These effects on the average spectra are attributed to physical intermixing of Au and Ag at the interface which would contribute to spectra with different barrier heights being included in the average spectra. Evidence of both Au and Ag at the interface for both silver samples was confirmed with XPS and RBS depth profiling and is consistent with the complete miscibility of Ag/Au, which would account for diffusion of Au to the interface [29].

A better view of the effects of this mixing on the electrostatic character of the interface

can be seen in the SBH histograms and maps. The standard deviation of the histogram of the SBH in the Au sample is 24 meV. In comparison, the SBH histograms of both silver samples show highly asymmetric distributions that are about four times broader. In addition, the 1 nm silver sample has a secondary peak near 0.7 eV. The SBH spatial maps of the silver samples show the physical grouping of the high and low barrier heights, which would be consistent with multiple species at the interface.

The Schottky barrier height histograms for the silver samples can be utilized to quantify the intermixing at the interface and compare to the metrology results. The approach taken is to sum multiple Gaussians into one that fits the envelope of the histogram and then compute the area under each Gaussian and assign it to a species; Au, Ag, or defects. It was found that five Gaussians were needed to form a fitting envelope, two for each species and one for defects as seen in Fig. 5. The two for each species are attributed to pinch-off effects due to the presence of different metals in close proximity to one another [9–12]. Periodically sampling over an array of patches as in this study, will result in several barrier heights in between that of pure Au (0.84 eV) and pure Ag (0.66 eV) [25]. Calculations indicate that the change in the local barrier height between a circular patch of Ag surrounded by Au transitions smoothly from the center of a silver patch to the edge, which is supported with the experimental observation by Olbrich et al. and Sirringhaus et al. [15, 16, 18]. For an array of circular patches surrounded by and infinite area of gold, numerical calculations indicate that the barrier height inside and outside a circular silver patch is lower than for an isolated patch. In addition, defects and/or foreign species will result in measuring higher barrier heights such as those from oxides or simply from increased scattering [18].

For the 30 nm Ag sample, the curves above 0.85 eV are attributed to both defects and gold. The relative area under the fits to these peaks is 18.5%, putting an upper bound on the presence of defects and gold. The area under the three curves below 0.85 eV are attributed to Ag. Utilizing the perturbation equation for a single circular SBH inhomogeneity measured at its center, it is found that these barrier heights correspond to isolated silver patches with radii of 200 nm and 400 nm, respectively as displayed in the insets of Fig. 5 [9–12]. These sizes are larger than the sizes of the regions in the maps, but are in agreement with the close proximity of the patches. The lowest peak is attributed to silver. The amount of silver at the interface is approximated by the sum of the three lower peaks of 81.5%.

Applying similar analysis to the peaks of the 1 nm Ag sample indicates Au as the domi-

nant species at the interface by computing the area under the peaks above 0.85 eV. The peak around 0.85 eV is considerably narrow indicating that the contributions due to gold are in excess of 58%. The large overlap between the peak centered at 0.85 eV and 0.75 eV indicate that the latter peak has contributions from both Au and Ag. The lowest two peaks are contributed to by almost silver exclusively. These barrier heights are lower than expected from the electrostatic model for a single patch, and are attributed to the close proximity of the patches and a high level of intermixing of the species. The amount of silver at the interface is again the sum of the three lower peaks of 26.5%.

These BEEM estimates are consistent with the XPS data, which shows silver composition of about 90% and 15% at the interface for the 30 nm Ag and 1 nm Ag samples, respectively. The BEEM and XPS estimates are also consistent with the large difference in the amount of silver between both samples. The silver in 1 nm sample is most likely not a full layer and would easily allow for Au at the interface. The Au present at the interface in the 30 nm thick silver is attributed to diffusion and the miscibility of Au and Ag.

## V. CONCLUSION

The Schottky barrier height inhomogeneities in mixed Au/Ag/Si(001) diodes has been mapped to nanoscale dimensions using BEEM. The average BEEM spectra and fits indicate that a single threshold model cannot capture the complex mixing occurring at these interfaces. These results show that SBH maps and histograms are needed to gain insight into these mixed interfaces, where fits to the histograms are utilized to estimate the relative amount of species present at the interface and are consistent with the chemical composition of the interface observed with XPS and RBS. These findings demonstrate a method to infer interface composition from the interface electrostatic properties as measured with BEEM.

## VI. ACKNOWLEDGMENTS

The authors acknowledge the support of the Semiconductor Research Corporation, Center for advanced Interconnect Science and Technology, and the National Science Foundation Grant DMR-1308102, and SEMATECH.

- 
- [1] H. Nienhaus, H. S. Bergh, B. Gergen, A. Majumdar, W. H. Weinberg, and E. W. McFarland, *Appl. Phys. Lett.* **74**, 4046 (1999).
- [2] X. Li, H. Zhu, K. Wang, A. Cao, J. Wei, C. Li, Y. Jia, Z. Li, X. Li, and D. Wu, *Adv. Mater* **22**, 2743 (2010).
- [3] M. Nishisaka, S. Matsumoto, and T. Asano, *Jpn. J. Appl. Phys.* **42**, 2009 (2003).
- [4] B. E. Coss, P. Sivasubramani, B. Brennan, P. Majhi, R. M. Wallace, and J. Kim, *J. Vac. Sci. Technol. B* **31**, 021202 (2013).
- [5] S. Smith, K. Aouadi, J. Collins, E. van der Vegt, M.-T. Basso, M. Juhel, and S. Pokrant, *Microelectron. J.* **82**, 261 (2005).
- [6] S. Haimsona, Y. Shacham-Diamand, D. Horvitz, and A. Rozenblat, *Microelectron. Eng.* **92**, 134 (2012).
- [7] F. Papadatos, K. Wong, V. Arunachalam, C. H. Shin, Z. Li, M. Chudzik, W.-H. Lee, and A. Xing, *Microelectron. Eng.* **92**, 2012 (123).
- [8] M. Tsai, H. Chao, L. Ephrath, B. Crowder, A. Cramer, R. Bennett, C. Lucchese, and M. Wordeman, *J. Electrochem. Soc.* **128**, 2207 (1981).
- [9] R. T. Tung, *Mater. Sci. Eng. R Rep.* **35**, 1 (2001).
- [10] R. T. Tung, *Phys. Rev. B* **45**, 509 (1992).
- [11] R. T. Tung, *J. Vac. Sci. Technol. B* **11**, 1546 (1993).
- [12] R. T. Tung, *Phys. Rev. Lett.* **84**, 6078 (2000).
- [13] C. Detavernier, R. L. Van Meirhaeghe, R. Donaton, K. Maex, and F. Cardon, *J. Appl. Phys.* **84**, 3226 (1998).
- [14] G. M. Vanalme, L. Goubert, R. L. V. Meirhaeghe, and F. C. and P Van Daele, *Semicond. Sci. Technol.* **14**, 871 (1999).
- [15] A. Olbrich, J. Vancea, F. Kreupl, and H. Hoffmann, *J. Appl. Phys.* **83**, 358 (1998).
- [16] A. Olbrich, J. Vancea, F. Kreupl, and H. Hoffmann, *Appl. Phys. Lett.* **70**, 2559 (1997).
- [17] K. E. J. Goh, A. Bannani1, and C. Troadec, *Nanotechnology* **19**, 445718 (2008).
- [18] H. Sirringhaus, T. Meyer, E. Y. Lee, and H. von Känel, *Phys. Rev. B* **53**, 15944 (1996).
- [19] H. Palm, M. Arbes, and M. Schulz, *Phys. Rev. Lett.* **71**, 2224 (1993).
- [20] C. A. Durcan, R. Balsano, and V. P. LaBella, *J. Appl. Phys.* **116**, 023705 (2014).

- [21] H. Palm, M. Arbes, and M. Schulz, *Appl. Phys. A* **56**, 1 (1993).
- [22] L. D. Bell and W. J. Kaiser, *Phys. Rev. Lett.* **61**, 2368 (1988).
- [23] W. J. Kaiser and L. D. Bell, *Phys. Rev. Lett.* **60**, 1406 (1988).
- [24] M. H. Hecht, L. D. Bell, W. J. Kaiser, and L. C. Davis, *Phys. Rev. B* **42**, 7663 (1990).
- [25] R. Balsano, A. Matsubayashi, and V. P. LaBella, *AIP Advances* **3**, 112110 (2013).
- [26] J. J. Garramone, J. R. Abel, I. L. Sitnitsky, L. Zhao, I. Appelbaum, and V. P. LaBella, *Appl. Phys. Lett.* **96**, 062105 (2010).
- [27] J. J. Garramone, J. R. Abel, I. L. Sitnitsky, and V. P. LaBella, *J. Vac. Sci. Technol. A* **28**, 643 (2010).
- [28] M. Krause, A. Stollenwerk, C. Awo-Affouda, B. Maclean, and V. P. LaBella, *J. Vac. Sci. Technol. B* **23**, 1684 (2005).
- [29] S. H. Wei, A. A. Mbaye, L. G. Ferreira, and A. Zunger, *Phys. Rev. B* **36**, 4163 (1987).

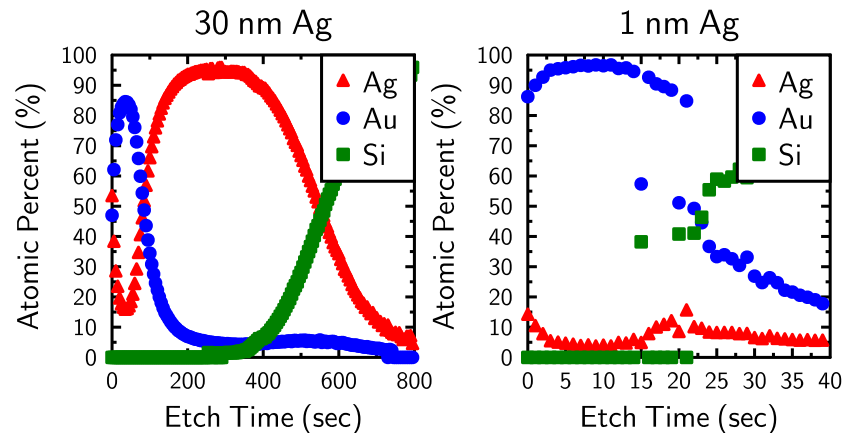


FIG. 1: Depth profiles from XPS data for the 7.5 nm Au /30 nm Ag/Si(001) (left) and 7.5 nm Au /1 nm Ag/Si(001) (right) diodes.

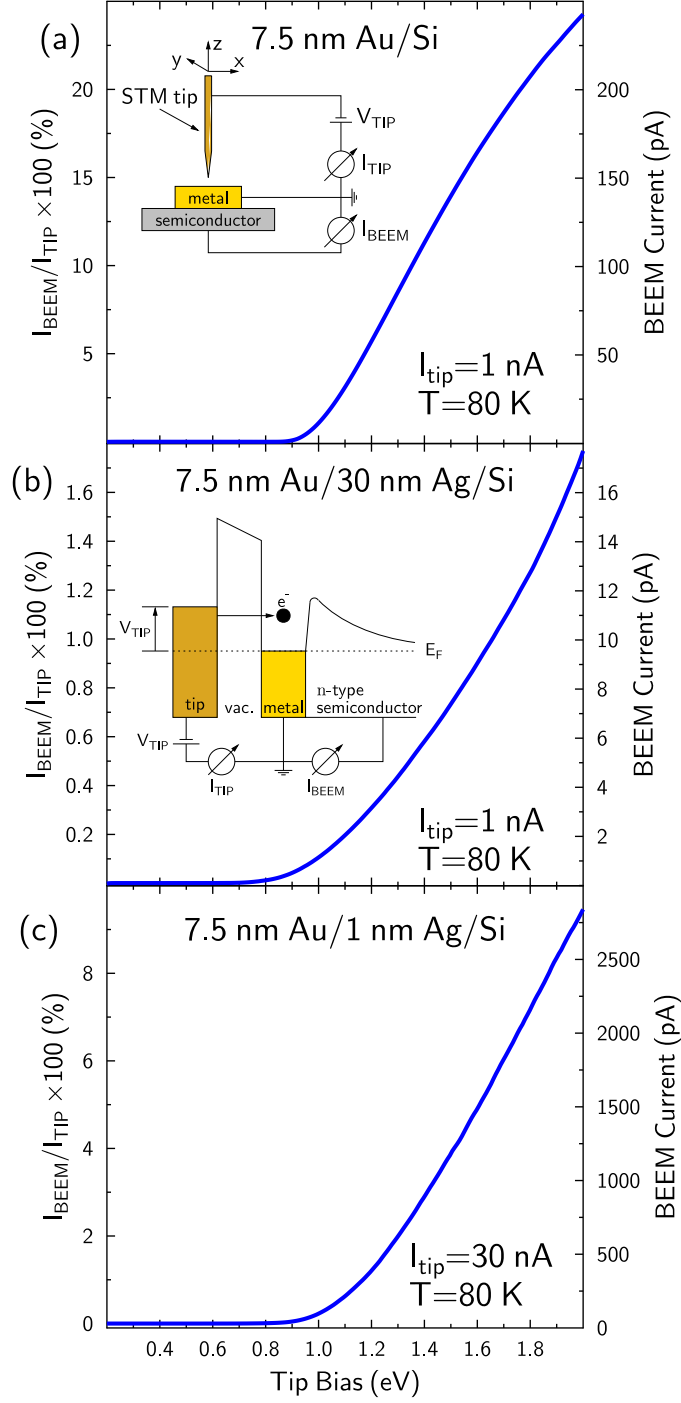


FIG. 2: Inset (a), the Schematic of the BEEM experiment, inset (b) band energy diagram of the BEEM experiment, the averaged BEEM spectrum of (a) 7.5 nm Au/Si(001) sample, (b) 7.5 nm Au/30 nm Ag/Si(001) sample, (c) 7.5 nm Au/1 nm Ag/Si(001) sample.

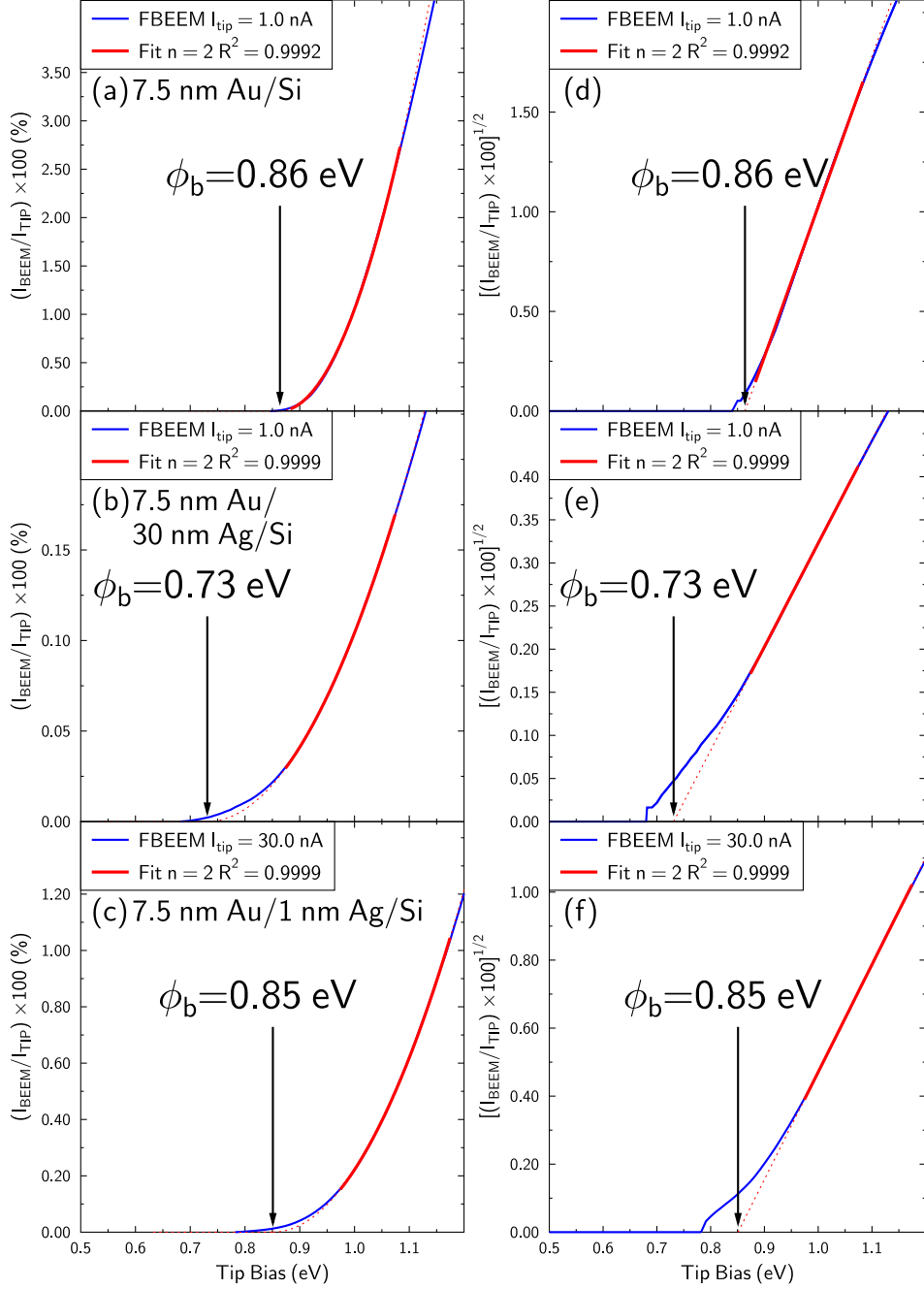


FIG. 3: The fits to averaged BEEM spectrum of plotted on a standard scale (a) 7.5 nm Au/Si(001) sample, (b) 7.5 nm Au/30 nm Ag/Si(001) sample, (c) 7.5 nm Au/1 nm Ag/Si(001) sample and plotted on as the square root of their values (d) 7.5 nm Au/Si(001) sample, (e) 7.5 nm Au/30 nm Ag/Si(001) sample, (f) 7.5 nm Au/1 nm Ag/Si(001) sample.

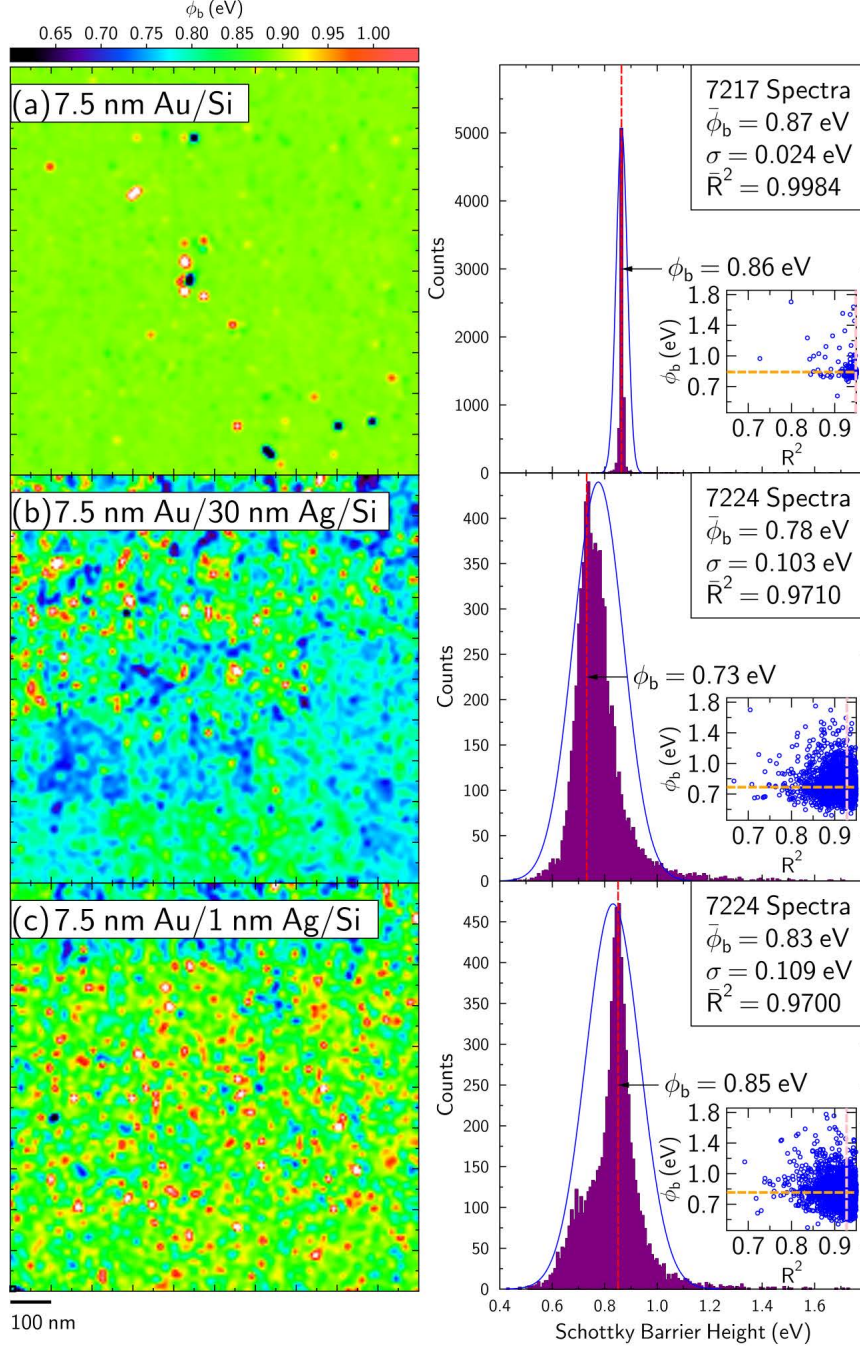


FIG. 4: False color maps of the SBHs as a function of position (left) and distribution histograms (right) for (a) 7.5 nm Au/Si(001) sample, (b) 7.5 nm Au/30 nm Ag/Si(001) sample, (c) 7.5 nm Au/1 nm Ag/Si(001) sample. The small box in the bottom left corner of the map in (c) indicates the pixel size. The red dotted line on the histograms indicate the SBH calculated from the averaged spectrum. A normal distribution is drawn around the data scaled for the size of the bins. Inset in the histograms, all SBHs for the same sample are plotted as a function of  $R^2$  value. The horizontal yellow dotted line indicates the average SBH value. The vertical pink dotted line indicates the average  $R^2$  value.

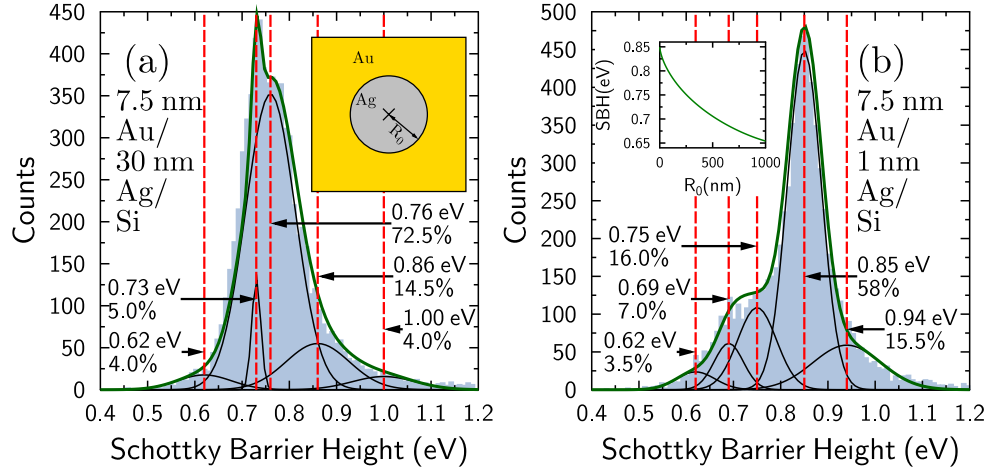


FIG. 5: The distribution of SBHs for the 7.5 nm Au/30 nm Ag/Si(001) (a) and the 7.5 nm Au/1 nm Ag/Si(001) (b) diodes with multi-modal fits indicated in green. Each normal distribution is shown in black and the mean SBH of each distribution indicated by a dotted red line. Inset in (a) is a schematic of the system modeled in the inset of (b), which displays the relationship between patch size and calculated SBH.